X-RAY AND NEUTRON INTERFEROMETRY

W. Graeff
Deutsches Elektronen-Synchrotron DESY
2000 Hamburg 52, Notkestrasse 85
Fed. Rep. of Germany

The extension of light optical interferometry to the Angström range required the development of new techniques for coherent beam splitting and handling since the refractive index for X-rays or matter waves like neutrons is too close to unity to allow the efficacious application of usual optical components.
Interferometry with such a small wavelength started with electrons. Marton et al.[1] tested in 1953 an interferometer composed of three separate crystal lamellae for beam splitting, deflection and superposition. Alignment and stability problems resulting in a rather poor interference contrast did not encourage to follow up this way. One year later Möllenstedt and Düker[2] therefore used the principle of Fresnel's biprism interferometer to realize the first electron interferometer with electrostatic lenses. Again Fresnel's biprism arrangement was chosen for the first attempt to neutron interferometry made by Maier-Leibnitz and Springer[3] in 1962. The very small beam separation of about 60 μm made the insertion of a sample rather difficult.
In 1965 Bonse and Hart[4] developed the first powerful interferometer in the Angström range with X-rays. They solved the problem of the Marton interferometer by making the three crystal lamellae out of the same perfect crystal leaving a rigid connection between the crystal slabs. The coherent beams were widely separated and easily accessible to macroscopic samples. A similar perfect crystal interferometer marked in 1974 the break through of neutron interferometry (Rauch, Treimer, Bonse).[5]
During this lecture we want to restrict ourselves to the discussion of this interferometer type. A description of other interferometer designs may be found in one of the recent review articles and workshop proceedings[6,7,8]. Furthermore, due to space limitations it is not possible to give a detailed reference list which may be found in [7] and [8].

The perfect crystal interferometer

Working principle

The geometry of components and beam paths is sketched in Fig. 1. The incoming wave is split, deflected and superposed through three consecutive Bragg reflections within the perfect crystal lamellae. This arrangement is known as triple Laue case (LLL) interferometer.

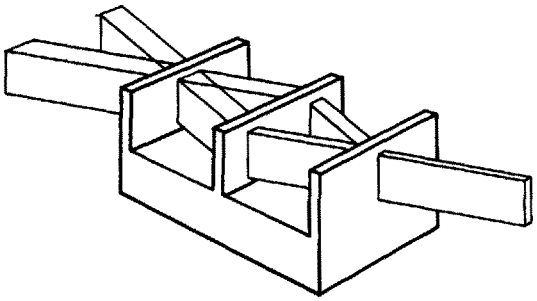

Fig. 1:
Triple Laue case interferometer made out of a perfect single crystal.

The superposition of the two coherent waves in front of the last crystal lamella, the so-called analyzer, forms a standing wave pattern with the same spacing as the reflecting net planes. Its relative position determines the intensities in the outgoing beams.

The theory of the LLL interferometer dealing both with incident plane and spherical waves can be found in the literature[7,9]. With perfect crystals dynamical theory has to be applied. As this theory is subject of a different lecture we only mention that for every incident plane wave two internal propagation modes, the so-called wavefields, are excited. Their slightly different wave vectors cause a beating of the intensity in the outgoing beams known as Pendellösung effect[10]. For a single reflection and without absorption, as it is the case with thermal neutrons in silicon, the intensity T of the transmitted and R of the reflected beam are complementary and have a constant sum, the incident intensity (here set to 1).

The values of T and R strongly depend on angle of incidence and crystal thickness. A quick calculation shows that the intensities of the interfering beams are in forward direction (0-beam) $T_S R_M R_A$ and $R_S R_M T_A$ but for the diffracted direction (h-beam) $T_S R_M T_A$ and $R_S R_M R_A$. For maximum interference contrast we find the conditions of ideal geometry:

(a) parallel setting of all crystal components (in most cases guaranteed by the common base)
(b) focussing of the coherent beams on to the entrance surface of the third crystal
(c) equal thickness of first and third crystal lamella.

Interference contrast

If these conditions are met the 0-beam theoretically has always 100 % interference contrast whereas the h-beam has an averaged contrast of 43 % with no absorption and all three lamellae equally thick. With increasing absorption the Pendellösung effect

vanishes and with strong absorption ($\mu t >> 1$) the Borrman effect (anomalous transmission) dominates. Here the R- and T-curves nearly coincide so that condition (c) can be omitted and the contrast in the h-beam can reach 100 %, as well.
Simply speaking with low absorption a phase shift in one partial beam switches the intensity from one outgoing beam to the other (with an incoherent background in the h-beam) whereas with high absorption a phase shift switches between anomalously high and low transmission through the analyzer for both outgoing beams. In the intermediate range (μt = 0.3 - 0.4) the contrast in the h-beam can even drop to 10 %.

Geometrical tolerances

Deviations from the ideal geometry may occur with different crystal thicknesses of splitter and analyzer or different gap widths between the crystals. The latter results in a defocussing Δz of the partial beams. With low absorption a tolerable value of Δz is $\Delta_e/6$ where Δ_e is the extinction length. With high absorption the incident spherical wave gets more and more a plane wave and $\Delta z \approx \Delta_e$ may be tolerated. But this does not help so much because with increasing absorption the extinction length at least with X-rays decreases.
Absolute values of the defocus Δz which causes 50 % loss of contrast range between 10 and 16 μm[7].

Applications

The interferometer as a sample

As already mentioned a misfit in either spacing or position of the standing wave pattern in front of the analyzer and the netplanes inside alters the intensity of the outgoing beams analogue to the moirê technique used in optics for comparison of two similar gratings. Hence the interferometer is a very sensitive tool to detect minute strains and misorientations in one of the crystal components.
This technique was used to study inhomogeneous distributions of point defects, strain fields of single dislocations and dislocation aggregates, radiation damage due to ion implantation and stresses exerted by a thin metal film evaporated on the analyzer.

Absolute lattice parameter determination

By shifting the analyzer crystal with respect to the rest of the interferometer sideways every passage of one net plane corresponds to one oscillation period of the outgoing intensity. Thus simply by counting fringes and measuring the total shift with a light optical interferometer directly operated with the length standard lamp it was possible to establish a secondary standard in the Angström range with an accuracy of better than 10^{-6} (Deslattes et al., 1974)[11].
With such a standard at hand the redefinition of Avogadro's constant, several ratios of fundamental constants involving Planck's constant and the recalibration of γ-ray reference lines are possible.

Determination of refractive index

Measuring the refractive index of a sample is the obvious task in interferometry. For X-rays the refractive index is directly related to the forward scattering factor f(o) and for neutrons to the coherent scattering length b_c.[12]
The interesting part of the scattering for X-rays is the anomalous dispersion correction f' in the neighbourhood of absorption edges. The exact knowledge of f' with varying wavelength is important for phase determination in crystallography. Furthermore the short wavelength side of the absorption edge displays a fine structure which is closely related to the structure of absorption spectra, known as EXAFS. Such measurements have both been made with synchrotron radiation[13] (see Fig. 2) and Bremsstrahlung radiation.

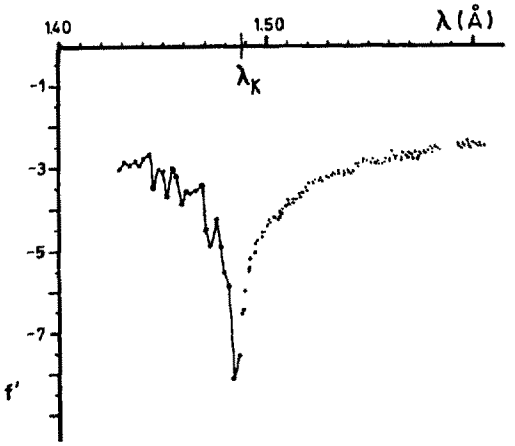

Fig. 2

Anomalous dispersion correction f' for Ni near the K-edge (courtesy G. Materlik)

For neutrons three kinds of interactions are traceable with interferometric methods: the nuclear scattering, the magnetic interaction (if present) with the electron shell and to some extent the Foldy interaction between the atomic Coulomb field and the charge distribution of the neutron. Besides the measurements of the forward directed scattering for a variety of solid, liquid and gaseous samples experiments have been performed with crystalline samples near Bragg reflection to reveal the change in refractive index described by the dispersion surface in dynamical theory[14] (see Fig. 3).

The quantities f and b_c are determined via the measurement of the λ-thickness t_λ of a sample. (A plate of thickness t_λ shifts the phase of a transmitted wave about 2π). In addition the wavelength, the density and the sample thickness must be known with sufficient precision. The precision of t_λ-measurements is of the order of 10^{-3}. Phase shifts are induced either by rotation of a plane parallel sample[15] or by moving the sample in and out and detecting the phase shift by means of the scanning interferometer[16] where the analyzer is shifted sideways. By working simultaneously at two wavelengths the sample geometry can even be eliminated.

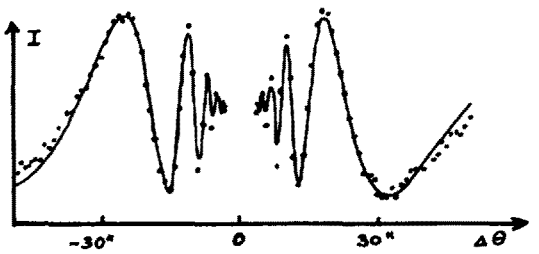

Fig. 3:
Interference pattern caused by rotating a perfect Si sample inside the interferometer through a Bragg reflection.

Phase contrast topography

By inserting a sample in the interferometer and detecting the outgoing beams on high resolution photographic film, in case of neutrons an additional converter like Gd is necessary, a direct phase contrast image is obtained, provided the absorption length $t_a = \mu^{-1}$ is much larger than the λ-thickness t_λ of the material under consideration. This is true for X-rays and light elements and might be useful for imaging of biological samples as it was demonstrated by Ando and Hosoya[17].

In case of thermal neutrons the condition $t_\lambda << t_a$ is quite often encountered. In addition phase contrast may be obtained from magnetically ordered regions in the sample. Experiments on neutron phase contrast imagery are under way[18].

Special experiments with neutrons

Two experiments should be mentioned which aimed at the particle properties of the neutron, namely its spin and mass. From quantum mechanics it is known that a spinor wave function of a spin 1/2 particle produces a phase factor -1 under 2π rotation, hence has a 4π-periodicity. This could clearly be demonstrated in several interferometric experiments[19].
Another experiment performed by Colella et al.[20] impressively showed the sensitivity of interferometric methods. They measured the phase difference of two coherent neutron beams travelling in earth's gravitational potential a few centimeters apart.
Suggestions have been made to use the scanning interferometer as a high frequency neutron chopper[21] for neutron spectroscopy. Chopping rates of 10 to 100 MHz seem feasible.

Summary

Since the invention of the perfect crystal interferometer X-ray and neutron interferometry have found a widely spread field of applications. Scattering factors for X-rays and coherent scattering lengths for neutrons are measured with high precision. Experiments answering questions in fundamental physics, metrology, crystallography and material science, as well, have been performed.
Theories have been developed to predict intensity profiles of the interfering beams, contrast and image formation for both absorbing and non-absorbing interferometers.

However, the influence of crystal quality on phase blurring and interference contrast needs some clarification.

References

1) L.A. Marton, J.A. Simpson, J.A. Suddeth: Phys. Rev. 90,410 (1953)
2) G. Möllenstedt, H. Düker: Naturwiss. 42, 41 (1954)
3) H. Maier-Leibnitz, T. Springer: Z. Physik 167, 386 (1962)
4) U. Bonse, M. Hart: Appl. Phys. Lett. 6, 155 (1965)
5) H. Rauch, W. Treimer, U. Bonse: Phys. Lett. 47A, 369 (1974)
6) M. Hart: Proc. Roy. Soc. A346, 1 (1975)
7) U. Bonse, W. Graeff:X-ray and Neutron Interferometry, in "X-Ray Optics", ed. H.J. Queisser (Springer Verlag Berlin Heidelberg New York 1977) pp. 93-143.
8) Proceedings of the Internat. Workshop on Neutron Interferometry, ed. by U. Bonse, H. Rauch (Oxford University Press, in press).
9) D. Petrascheck, R. Folk: phys. stat. sol. (a) 36, 147 (1976)
10) see also A. Authier in this volume
11) R.D. Deslattes, A. Henins, H.A. Bowman, R.M. Schoonover, C.L. Carrol, I.L. Barnes, L.A. Machlan, L.J. Moore, W.R. Shields: Phys. Rev. Lett. 33, 463 (1974)
12) See also L. Gerward, G. Squires, A. Steyerl in this volume
13) U. Bonse, G. Materlik: Z. Physik B24, 189 (1976)
14) W. Graeff, W. Bauspieß, U. Bonse, H. Rauch: Acta cryst. A34, S238 (1978)
15) W. Bauspieß, U. Bonse, H. Rauch: Nucl. Instrum. Meth. 157, 495 (1978)
16) C. Cusatis, M. Hart: Proc. Roy. Soc. A354, 291 (1977)
17) M. Ando, S. Hosoya: An Attempt at X-Ray Phase Contrast Microscopy, in Proc. of the 6th Int. Conf. on X-Ray Optics and Microanal., ed. by G. Shinoda, K. Kohra, T. Ichinokawa (University of Tokyo Press 1972) p. 63.
18) W. Graeff, W. Bauspieß, U. Bonse, M. Schlenker, H. Rauch: Acta Cryst. A34,S239 (1978).
19) H. Rauch, A. Wilfing, W. Bauspieß, U. Bonse:Z. Physik B29, 281 (1978)
S.A. Werner, R. Colella, A.W. Overhauser, C.F. Eagen: Phys. Rev. Lett. 35, 1053 (1975)
20) R. Colella, A.W. Overhauser, S.A. Werner: Phys. Rev. Lett. 34, 1472 (1975).
21) M. Hart: Multiple Wavelength Interferometry with X-Rays and Neutrons, in (8).